^{57}Fe-ion implantation in laser-deposited cupric and cuprous oxide films: Mössbauer spectroscopy and x-ray-diffraction studies

S. B. Ogale, P. G. Bilurkar, and S. Joshi
Centre for Advanced Studies in Materials Science and Solid State Physics, Department of Physics, University of Poona, Pune 411 007, India

G. Marest
Universite Claude Bernard Lyon 1 and IN2P3/CNRS, 43, Boulevard du 11 Novembre 1918, 69622 Villeurbanne, Cedex, France
(Received 28 March 1994; revised manuscript received 22 June 1994)

A systematic study of ^{57}Fe-ion implantation in cupric and cuprous oxide films has been reported. The CuO and Cu_2O films having excellent stoichiometry were prepared by the technique of laser ablation. The phases formed in the implanted and thermally annealed samples were characterized by Mössbauer spectroscopy and glancing angle x-ray diffraction. For the as-implanted CuO films the $Cu_6Fe_3O_7$, $CuFeO_2$, β-$CuFeO_2$, and Cu_2O phases are detected. The same phases are present in the Cu_2O-implanted films with some Cu_2O·FeO units, metallic Cu atoms, and $Cu_xFe_{3-x}O_4$ spinel in addition. Annealing at 400 °C under argon atmosphere produces in both the cases a strong increase of the $CuFeO_2$ and β-$CuFeO_2$ phases at the expense of the $Cu_6Fe_3O_7$ phase. This latter phase completely vanishes after annealing at 500 °C and new phases, namely α-Fe_2O_3 and small iron clusters appear. The amount of the $Cu_xFe_{3-x}O_4$ phase continues to increase after annealing at 500 and 600 °C, whereas $CuFeO_2$ decreases. The α-Fe_2O_3 contribution disappears after annealing at 600 °C.

INTRODUCTION

It is well established now, through several experimental and theoretical studies, that the Cu-O system configured in planar and chain-type coordinations is of central importance to the phenomenon of high-T_c superconductivity. It has also been found that in these systems there is a subtle boundary between the phenomena of antiferromagnetism and high-T_c superconductivity. It is believed that some intrinsic and specific features of the Cu-O system are crucial for the occurrence of these effects. Hence, considerable interest has grown in the understanding of binary compounds and related configurations based on the Cu-O system. One study, which is clearly expected to be useful in this context, is that of hyperfine interactions in such systems using powerful probes such as ^{57}Fe. The early ^{57}Fe Mössbauer studies on the Cu-O system have been reported by Cares and Hightower in the context of its performance as a catalyst for promotion of oxidative dehydrogenation.[1] It was argued that the ease of interconversion between Fe^{2+} and Fe^{3+} provides a reasonable oxidation-reduction pathway in this system for such reactions. Bhaduri has reported ^{57}Fe Mössbauer studies on the $Cu_xFe_{3-x}O_4$ system.[2] The objective of this study was to examine the influence of enhanced Cu content in the Fe_3O_4 matrix on the electron delocalization among the octahedral iron atoms. Mössbauer spectroscopy studies on the tetragonal and cubic $CuFe_2O_4$ ferrites have been reported by Janicki *et al.*[3] Hannoyer *et al.* have also studied the $Cu_xFe_{3-x}O_4$ system from the standpoint of revealing the two oxidation states of Fe and Cu in these ferrimagnets.[4] These authors have performed their studies at room temperature and at 4.2 K with and without strong applied magnetic fields and have shown that cubic $CuFe_2O_4$ is not completely inverse (spinel) and the degree of inversion depends on the heat treatment. This partial inversion has been identified to be the cause of distribution of hyperfine fields and the inhomogeneous broadening of the lines corresponding to octahedral sites in the Mössbauer spectra. Hannoyer *et al.* have also studied the effect of oxygen loss on the crystallographic and magnetic properties of $CuFe_2O_4$ ferrite.[5] By examining the correlation between the Mössbauer data, the data on unit-cell dimensions and electrical conductivity Bhaduri has shown that in the $Cu_xFe_{3-x}O_4$ system, for $x > 0.6$ the system behaves as a semiconductor as the sixth $3d$ electron of the Fe^{2+} ion becomes localized.[6] Gries, Sawicka, and Sawicki have investigated the internal oxidation behavior of Fe-implanted Cu (crystalline) sample subjected to annealing treatment in oxidizing atmosphere followed by oxygen-ion bombardment.[7] These authors have suggested that in the as-annealed-state quasimolecular units in the form of Cu_2O·FeO are formed wherein an octahedral position in the oxygen sublattice of Cu_2O is occupied by an Fe atom, it being substituted for two adjacent copper atoms. Since a stable phase of the type Cu_2FeO_2 has not been reported, it has been argued that a larger complex of such molecular units should be thermally unstable. Upon oxygen bombardment of the annealed-state delafossite ($Cu^+Fe^{3+}O_2^{2-}$) is found to be formed along with α-Fe_2O_3.

Niedermayer *et al.* have examined the antiferromagnetic order in CuO by Mössbauer source experiment in the context of its possible correlation with high T_c superconductivity.[8] Their Mössbauer data show presence of

0163-1829/94/50(14)/9743(9)/$06.00

antiferromagnetic ordering below $T_N = 226(1)$ K. Study of the temperature dependence of the electric quadrupole interaction is found to suggest a structural and/or charge-state transition near 150 K. Within 2 K of T_N these authors do not find any detectable line broadening of the Mössbauer spectra than can be attributed to $2d$ Heisenberg spin fluctuations as in the $La_{2-x}Sr_xCuO_4$ system. Smith *et al.* have also reported on Mössbauer and magnetic susceptibility studies on ^{57}Co-doped CuO.[9] Their Mössbauer spectra above 244 K show a dominant quadrupole-split site and at 244 K a line broadening of this dominant site has been observed indicating onset of local magnetic order. Similar results have been obtained by Barcs *et al.* for ^{57}Co:CuO samples: a doublet with a quadrupole splitting (QS) = 1.52 mm/s and a second doublet with QS = 2.49 mm/s; the relative abundance of the first doublet due to Fe^{2+} increasing with time at room temperature at the expense of the second doublet attributed to high spin Fe^{3+}.[10]

To prevent after effects due to the ^{57}Co nuclear decay ^{57}Fe isotope dopings were recently performed using two different processes. In the first process a target in the form of an ingot having 2 at. % ^{57}Fe mixed with Cu metal ingot was evaporated by an electron beam gun in oxygen atmosphere activated by radio-frequency plasma.[11] A paramagnetic doublet was observed above 180 K: isomer shift (IS) = 0.35 mm/s and QS = 1.37 mm/s were measured at room temperature. A significant broadening of this doublet below 150 K indicates that the magnetic ordering occurs in the temperature range between 150 and 180 K. The second process involves use of the nitrate route to prepare CuO-0.5 at. % ^{57}Fe. Again a paramagnetic spectrum was seen above 150 K.[12] The hyperfine parameters measured at room temperature (IS = 0.36 mm/s and QS = 0.84 mm/s) confirm that the valence of the doped ^{57}Fe in CuO is Fe^{3+}.

In the light of the fact that no coherent picture yet seems to have emerged about the attendant issues, we decided to perform ^{57}Fe Mössbauer spectroscopy studies on the Fe-Cu-O system, wherein precise quantities of ^{57}Fe are incorporated in CuO and Cu_2O matrices via ion implantation. One problem in such situation is the good stoichiometry of the starting material. We solved this problem by using the laser ablation technique, which has been very successful in the case of the deposition of high-T_c thin films of high-quality superconductors and other materials. We were able to deposit Cu_2O and CuO films of excellent stoichiometry using the pulsed laser ablation technique and such films were used in our studies.[13]

EXPERIMENT

Copper oxide pellets (1.5 cm diameter and 0.5 cm thick), used as the target materials for laser ablation, were prepared by pressing the cupric oxide (CuO) powder (99.99% pure) in the form of a pellet and sintering the pressed pellet at 500 °C for more than 2 h. Depositions were carried out in a vacuum chamber capable of yielding an ultimate background pressure of 10^{-5} Pa. A KrF excimer laser (wavelength $\lambda = 248$ nm and pulse width of 20 ns) was used for ablation. The laser beam was made incident on the target at an angle of 45°. The energy density at the target was fixed at 2.0 J/cm^2. The target was slowly rotated (10 rpm) during the deposition, in order to minimize texturing of its surface. The substrates were mounted in front of the target at a distance of 5 cm. The substrate temperature and oxygen pressure were optimized at two sets of values to achieve the desired stoichiometries in the film, namely, CuO or Cu_2O.[13] The samples were cooled to room temperature under the same ambient and same pressure that was fixed during deposition. Post deposition annealing treatment was also given to some of the samples in order to study their stability under thermal cycling.

The as-deposited samples were then characterized using bulk and glancing angle x-ray diffraction (XRD). After confirming their good structural and chemical quality such well characterized samples were ion implanted using 100 keV ^{57}Fe ions. It may be pointed out that the Cu_2O films were found to grow epitaxially due to the epitaxial compatibility of Cu_2O with MgO(100). Therefore, the surface normal of the Cu_2O samples was tilted at 10° with reference to the ion beam direction to avoid channeling during implantation. Both cupric and cuprous oxide samples were bombarded at two different values of ion doses, viz., 2×10^{16} ions/cm^2 and 5×10^{16} ions/cm^2. The ion-implanted samples were characterized by using conversion electron Mössbauer spectroscopy (CEMS) and grazing angle XRD techniques. The CEMS measurements were done using a ^{57}Co:Rh Mössbauer source mounted on a constant acceleration velocity transducer.[14] In addition to the use of a fitting procedure assuming Lorentzian line shapes, which allows hyperfine parameters to be determined (isomer shifts IS's, quadrupole splittings QS's, hyperfine fields B), a program elaborated by Le Caer and Dubois[15] was used to fit the hyperfine field distribution displayed by nonstoichiometric $Cu_xFe_{3-x}O_4$ phases. The glancing-angle XRD data were obtained using the Seeman Bohlin arrangement on a Rigaku machine model No. Rotaflex Ru 200 B.[16] The implanted samples were subjected to thermal annealing under Ar atmosphere at 400, 500, and 600 °C for 1 h.

RESULTS

As implanted samples

The glancing-angle x-ray-diffraction patterns (taken at $\alpha = 0.3°$) in the case of CuO films implanted with 100-keV $^{57}Fe^+$ ions at two fluence values are shown in (Fig. 1). The x-ray-diffraction pattern [Fig. 1(a)] of the sample implanted at a low fluence of 2×10^{16} ions/cm^2 indicates formation of Cu_2O, $CuFeO_2$, β-$CuFeO_2$ along with the $Cu_6Fe_3O_7$ phase. As the diffraction lines of these two last phases are very often overlapping, the existence of $Cu_6Fe_3O_7$ is not proved. No significant variation in phase formation was found after implantation at a high fluence of 5×10^{16} ions/cm^2 [Fig. 1(b)]. Once again the diffraction lines corresponding to Cu_2O, β-$CuFeO_2$, $CuFeO_2$, and $Cu_6Fe_3O_7$ phases are seen but with different relative intensities. The diffraction patterns taken at $\alpha = 0.5°$ (not shown) were found to be almost identical to

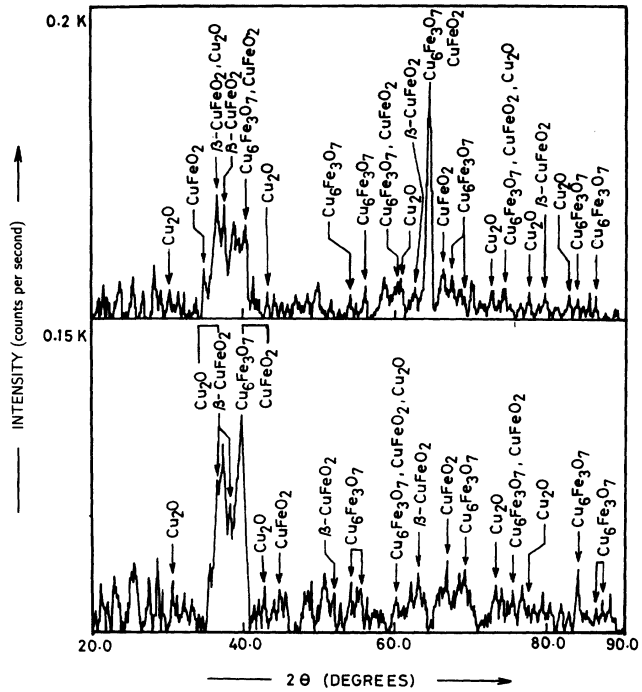

FIG. 1. Glancing-angle x-ray-diffraction pattern ($\alpha=0.3°$) for CuO films implanted with 100-keV ^{57}Fe ions at dose values of (a) 2×10^{16} ions/cm^2 and (b) 5×10^{16} ions/cm^2.

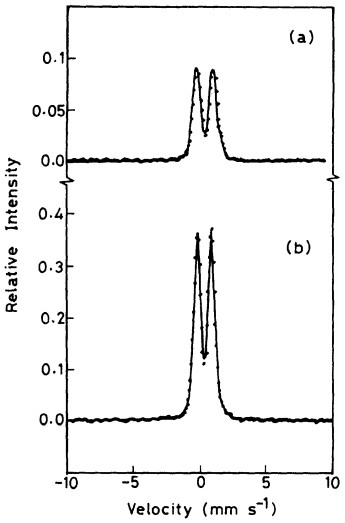

FIG. 2. CEM spectra for CuO films implanted with 100-keV ^{57}Fe ions at dose values of (a) 2×10^{16} ions/cm^2 and (b) 5×10^{16} ions/cm^2.

the pattern taken at $\alpha=0.3°$, whereas the intensity of the lines was found to decrease strongly for $\alpha=1°$ to vanish at $\alpha=5°$. At this glancing angle only CuO was detected. The variation of the intensities as a function of α reflects the depth distribution of the phases due to the Gaussian distribution of implanted iron atoms.[17]

The conversion electron Mössbauer (CEM) spectra for the CuO films implanted at 2×10^{16} and 5×10^{16} ions/cm^2 are shown in Fig. 2. The hyperfine parameters are summarized in Table I. The spectrum, which corresponds to the low fluence [Fig. 2(a)] can be fitted with two doublets $D1$ and $D2$ having identical isomer shifts (IS=0.35 mm/s) but with very different quadrupole splittings (QS=0.93 mm/s and QS=1.51 mm/s, respectively). The same values were measured for substitutional ^{57}Fe in CuO by Shah and Gupta[12] and by Sohma and Kawaguchi[11] when the local iron concentration was 0.5 at. % and 2 at. %, respectively. In our experiment, if a Gaussian distribution of ranges is assumed, the average atomic concentration of iron in implanted layers can be estimated to be 4 at. % and the two doublets would reflect different environments. However, in the light of the glancing-angle x-ray-diffraction results, the $Cu_6Fe_3O_7$ could be present. To our knowledge, no Mössbauer data is available on the $Cu_6Fe_3O_7$ phase. If this compound is present, then iron should exist under the Fe^{3+} and Fe^{2+} charge states. We took into account the possibility of a ferrous state in a different fit. This fit showed that the hyperfine parameters of $D1$ and $D2$ do not change (only the intensity of $D2$ decreases from 60 to 52 %) and a new

TABLE I. Hyperfine Mössbauer parameters of ^{57}Fe implanted CuO and Cu_2O films. Isomer shifts (IS's) are relative to iron metal, (QS) is the quadrupole splitting, W is the line width, and B is the hyperfine field.

Sample	IS (mm/s)	QS (mm/s)	W (mm/s)	B (T)	Contribution (%)
CuO-As	0.35	0.93	0.40		40
implanted at 2×10^{16} ions/cm^2	0.35	1.51	0.49		60
CuO-As implanted at 5×10^{16} ions/cm^2	0.32	1.05	0.52		100
Cu_2O-As	0.32	1.12	0.53		96
implanted at 2×10^{16} ions/cm^2	1.09	2.12	0.24		4
Cu_2O-As	0.32	1.02	0.84		49
implanted at	1.09	1.80	0.90		5
5×10^{16} ions/cm^2	0.39	−0.12	1.03	43	29
	0.51	0.00	1.10	35	17

doublet (IS=0.81 mm/s, QS=1.45 mm/s) with a rather low abundance (6%) is present. This doublet would be the signature of Fe^{2+} but with a rather low intensity. A third hypothesis can be proposed to explain the doublets $D1$ and $D2$. As proposed by Shah and Gupta, $D1$ would represent substitutional iron in CuO, whereas $D2$, which has a higher quadrupole splitting, could reflect the presence of a very badly crystallized delafossite due to the defects created by the implantation process.

At the higher fluence value of 5×10^{16} ions/cm^2, no change in the general nature of the CEM spectrum is observed [Fig. 2(b)]. The corresponding spectrum can be fitted with only one doublet (IS=0.32 mm/s, QS=1.05 mm/s), whose parameters closely match with those of doublet $D1$. Expecting the existence of the $Cu_6Fe_3O_7$ phase, another fit was attempted, which gave IS=0.28 mm/s, QS=0.85 mm/s with a relative intensity (RI)=38% for the doublet $D1$. In this fit the values of the hyperfine parameters for the two doublets were (IS=0.26 mm/s, QS=1.26 mm/s, RI=44%) and (IS=0.54 mm/s, QS=1.08 mm/s, RI=17%). The $Cu_6Fe_3O_7$ phase can be expressed as $3Cu_2O$-Fe_3O_4. It is worthy to note that the isomer shifts corresponding to Fe^{3+} and the mixed valence $Fe^{2.5}$ are similar to the isomer shifts of tetrahedral and octahedral sites in Fe_3O_4.

As stated earlier the cuprous oxide films, which were grown on (100) MgO were epitaxial in nature, and, as such, during implantation they were tilted at an angle of 10° with respect to the ion beam to avoid channeling of the incident ions. X-ray-diffraction patterns for the Cu_2O films implanted at 2×10^{16} ions/cm^2 and 5×10^{16} ions/cm^2 recorded at the glancing angle of 0.3° are shown in Fig. 3. Both the patterns show different diffraction lines corresponding to $CuFeO_2$, β-$CuFeO_2$ phases along with those for the $Cu_6Fe_3O_7$ phase. Few diffraction lines corresponding to the Cu_2O phase can also be seen. Cu_2O was found to be mainly located at the surface, since in the XRD patterns taken at higher angles of incidence (results not shown) these diffraction lines were found to be absent. In the case of high-dose-implanted sample some lines due to metallic Cu could also be observed.

The CEM spectrum for the Cu_2O film implanted at low dose [Fig. 4(a)] could again be fitted with two doublets, one of which could be identified with the doublet $D1$ previously discussed. The other doublet, which has a contribution of only 4% has hyperfine parameters IS=1.09 mm/s and QS=2.12 mm/s. The CEM spectrum corresponding to the case of high-dose implantation (5×10^{16} ions/cm^2) in Cu_2O, shown in Fig. 4(b), can be resolved into the same two doublets as well as two additional sextets. The two magnetically split six-line patterns with mean hyperfine fields (B) values of 43 and 35 T can be attributed to spinel $Cu_xFe_{3-x}O_4$. Their low values and the very broad distribution of hyperfine field indicate that x is in the range 0.6–0.8.[12,18]

Annealed samples

In order to study the phase evolution upon thermal annealing, the ion implanted samples were heat treated under argon atmosphere at different temperatures for 1 h.

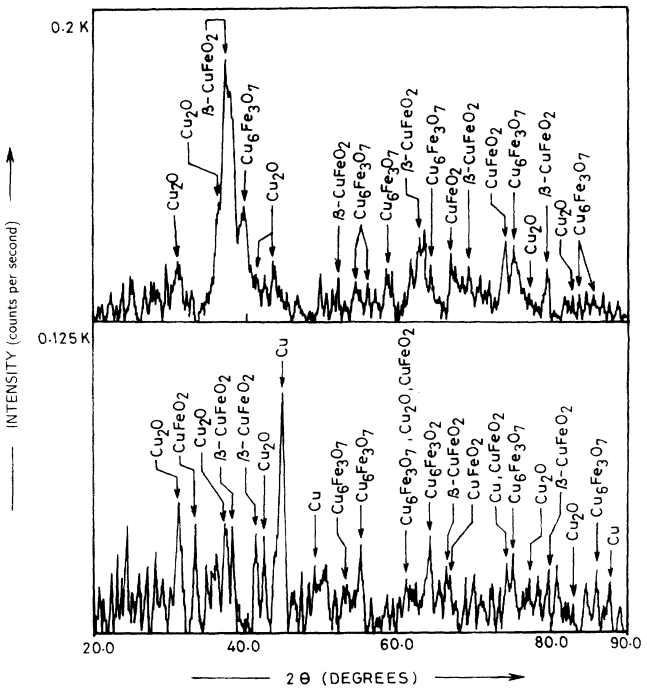

FIG. 3. Glancing-angle x-ray-diffraction pattern ($\alpha=0.3°$) for Cu_2O films implanted with 100-keV ^{57}Fe ions at dose values of (a) 2×10^{16} ions/cm^2 and (b) 5×10^{16} ions/cm^2.

The hyperfine parameters used to fit the CEM spectra (not shown) for the annealed samples are summarized in Tables II and III. The x-ray-diffraction data (not shown) were also recorded and the corresponding results were compared with the Mössbauer results.

It is observed from both the CEMS and XRD data that in the CuO sample implanted at 2×10^{16} ions/cm^2 after annealing at 400 °C there is a reduction in the contribution due to $Cu_6Fe_3O_7$ phase with a concomitant increase in the contributions of Cu_2O, $CuFeO_2$, and β-$CuFeO_2$

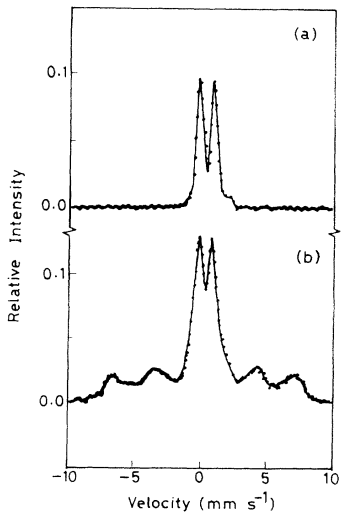

FIG. 4. CEM spectra for Cu_2O films implanted with 100-keV ^{57}Fe ions at dose values of (a) 2×10^{16} ions/cm^2 and (b) 5×10^{16} ions/cm^2.

phases. No new phases are detected. The CEM spectrum in this case could be fitted again with the doublet $D1$ and a new doublet $D2$ having hyperfine parameters as IS=0.38 mm/s, QS=0.64 mm/s corresponding (without any ambiguity) to the $CuFeO_2$ phase.[19] The contribution of this new phase is very significant (82%); it can possibly be attributed to the decomposition at 400 °C of $Cu_6Fe_3O_7$ phase and to the oxidation of iron located in substitutional sites. This result was found to be consistent with the corresponding x-ray-diffraction results, wherein reduction in the diffraction peak intensities attributed to this phase could be seen. For the CuO sample implanted at 5×10^{16} ions/cm^2, this decomposition is found to be even more pronounced as the corresponding Mössbauer data showed the presence of only $CuFeO_2$ phase. After annealing at 500 °C the $CuFeO_2$ phase remains to be the major phase, $Cu_6Fe_3O_7$ phase disappears completely and new phases appear. The additional singlet seen in this case can be attributed to segregation of fine Fe particles in the film. Local epitaxy of α-Fe on released free grains of fcc copper cannot also be ruled out. The glancing-angle x-ray-diffraction patterns of the corresponding films, did not show any diffraction lines due to Fe phase. Thus, if present, such clusters are expected to be less than a few nanometers in size. In addition to the iron precipitates a weak and broad magnetic distribution is seen to be present. This distribution could be divided into two parts using the Le Caer program.[15] The first magnetic component having hyperfine parameters IS=0.37 mm/s, B=51.8 T, and QS=−0.36 mm/s is characteristic of α-Fe_2O_3. Its relative intensity is only 1–2 %. The second component characterized by a very broad $p(B)$ distribution is attributed to the $Cu_xFe_{3-x}O_4$ phase. This last phase becomes predominant after annealing at 600 °C (43 [35+8] % and 53% for 2 and 5×10^{16} ions/cm^2, respectively), whereas α-Fe_2O_3 disappears and $CuFeO_2$ strongly decreases. At this high temperature a new nonmagnetic component with a very large QS had to be introduced in the fits. It corresponds to Fe^{3+} ions located in very distorted environments. The evolutions of $Cu_6Fe_3O_7$, $CuFeO_2$ and $Cu_xFe_{3-x}O_4$ as seen from the CEM data were once again found to be in agreement with the results of XRD measurements. Additionally, small contributions due to Cu_2O and metallic Cu (phases not accessible to ^{57}Fe Mössbauer spectroscopy) could also be discerned from XRD data.

The hyperfine parameters for the implanted Cu_2O samples annealed at 400, 500, and 600 °C are summarized in Table III. After annealing at 400 °C the doublet due to Fe^{2+} species is seen to vanish completely, the $Cu_6Fe_3O_7$ contribution strongly decreases and the $CuFeO_2$ and $Cu_xFe_{3-x}O_4$ phases appear. Appearance of such phases could also be confirmed by the x-ray-diffraction results. For the sample implanted with 2×10^{16} ions/cm^2 α-Fe_2O_3

TABLE II. Mössbauer parameters of the CuO films implanted with iron and then annealed at 400, 500, and 600 °C under argon atmosphere. * means that the component displays a distribution of hyperfine fields.

Sample (CuO)	IS (mm/s)	QS (mm/s)	W (mm/s)	B (T)	Contribution (%)
Implanted	0.38	0.64	0.26		82
2×10^{16} ions/cm^2	0.36	0.97	0.38		18
annealed at 400 °C					
Implanted	0.40	0.68	0.28		74
2×10^{16} ions/cm^2	−0.07	0.00	0.53		10
annealed at 500 °C	0.37	−0.36	0.40	51.8	2
	0.33	0.00	0.60	47.0	14
Implanted	0.40	0.69	0.32		38
2×10^{16} ions/cm^2	−0.08	0.00	0.47		7
annealed at 600 °C	0.27	1.8	0.82		12
	0.28	0.00	0.63	*41–46	35
	0.63	0.00	1.00	29.5	8
Implanted	0.37	0.67	0.39		100
5×10^{16} ions/cm^2					
annealed at 400 °C					
Implanted	0.39	0.68	0.28		76
5×10^{16} ions/cm^2	0.00	0.00	0.52		17
annealed at 500 °C	0.37	−0.36	0.42	51.8	1
	0.44	0.00		*42.4	6
Implanted	0.40	0.68	0.24		35
5×10^{16} ions/cm^2	−0.09	0.00	0.27		5
annealed at 600 °C	0.34	2.18	0.58		7
	0.27	0.00		*38–46	53

TABLE III. Mössbauer parameters of the Cu_2O films implanted with iron and then annealed at 400, 500, and 600 °C under argon atmosphere. * means that the component displays a distribution of hyperfine fields.

Sample (Cu_2O)	IS (mm/s)	QS (mm/s)	W (mm/s)	B (T)	Contribution (%)
Implanted	0.32	0.64	0.26		82
2×10^{16} ions/cm^2	0.37	0.97	0.38		18
annealed at 400 °C	0.37	−0.32		50.8	15
	0.59	0.00		*44.8	19
Implanted	0.40	0.68	0.28		74
2×10^{16} ions/cm^2	−0.07	0.00	0.53		10
annealed at 500 °C	0.37	−0.36	0.32	51.1	16
	0.29	0.00		*46.2	28
Implanted	0.40	0.66	0.23		89
2×10^{16} ions/cm^2	−0.07	0.00	0.22		11
annealed at 600 °C					
Implanted	0.34	1.00	0.85		4
5×10^{16} ions/cm^2	0.38	0.63	0.33		28
annealed at 400 °C	0.31	0.00	0.50	48.4	25
	0.58	0.00		*45.0	43
Implanted	0.40	0.67	0.23		77
5×10^{16} ions/cm^2	−0.03	0.00	0.23		7
annealed at 500 °C	0.41	−0.15	1.10	52.4	8
	0.36	0.00	0.51	*46.5	8
Implanted	0.40	0.69	0.27		48
5×10^{16} ions/cm^2	−0.01	0.00	0.79		7
annealed at 600 °C	0.37	1.85	0.91		15
	0.38	−0.35	0.95	50.8	5
	0.33	0.00	0.37	43.3	25

(15%) is also detected. This phase is present for the two samples annealed at 500 °C. At this temperature $Cu_6Fe_3O_7$ is completely decomposed and the $CuFeO_2$ phase becomes the main component. Although the magnetic phases are abundant for the sample implanted at 2×10^{16} ions/cm^2, these phases have decreased strongly for the sample implanted at 5×10^{16} ions/cm^2. For the two fluences, small fine iron precipitates appear as is the case for the CuO samples. After annealing at 600 °C only $CuFeO_2$ and Fe precipitates remain for the low-dose-implanted sample, whereas $Cu_xFe_{3-x}O_4$ increases again for the high-dose-implanted sample. It is worthy to note that the doublet due to Fe^{3+}, seen in the CuO samples, exists also in this sample in a non-negligible (15%) amount.

The x-ray-diffraction patterns also showed that $CuFeO_2$ and Cu_2O phases increase at the expense of $CuFe_2O_4$. Moreover, $CuFeO_2$ grows preferentially at the surface, whereas Cu_2O is mainly located in the deep layers. This was confirmed from the studies of patterns recorded at different glancing angles. After annealing at 600 °C the Cu_2O phase was observed with some amount of $CuFeO_2$ in the low-dose-implanted sample. For the high-dose-implanted sample the diffraction lines attributed to $CuFeO_2$ and $CuFe_2O_4$ were found to be narrower than after annealing at 500 °C. In this case, CuO could be clearly distinguished, chiefly when the glancing angle α was increased.

DISCUSSION

The results obtained in this work are required to be analyzed in terms of (1) the known phases of the ternary Cu-Fe-O system, the binary Cu-O and Fe-O systems and the elemental Cu, Fe, as well as Fe-Cu alloy states; (2) possible known consequences of the implantation process such as defect formation, freezing in of metastable states and/or phases, disturbance of the stoichiometry via loss of atomic constituents, etc., and (3) implications of annealing treatments for the evolution of the implantation-induced state into a state comprising of a combination of the known stable states, which can be configured from the attendant metastable states. The phases of the Cu-Fe-O ternary system, which have been studied in the past include $CuFe_2O_4$, $Cu_xFe_{3-x}O_4$ ($x=0.0$–0.89), $CuFeO_2$ (α and β states), and $Cu_6Fe_3O_7$. While detailed information about x-ray and Mössbauer data is available about the first three types of phases; no Mössbauer data is available on the $Cu_6Fe_3O_7$ system, to the best of the knowledge of the authors. Since the Mössbauer spectra for the as-implanted state in our samples invariably had a

doublet, which could not be identified with known Cu-Fe-O phases and, since the x-ray data on the same samples showed lines corresponding to $Cu_6Fe_3O_7$ phase, we have concluded that the parameters of the unidentified doublet should correspond to the state of the Fe atoms in the $Cu_6Fe_3O_7$ phase. It has been reported that in terms of powder spacings and other properties the $Cu_6Fe_3O_7$ phase is found to be identical to the delafossite phase ($CuFeO_2$); however, the calculated density is much higher than that measured for the delafossite phase.[20] It is interesting to note that the typical value of the isomer shift of the doublet that we have assigned to $Cu_6Fe_3O_7$ phase is 0.35 mm/s, which is close to the isomer shift value of 0.38 mm/s for the delafossite phase. The quadrupole splitting value of the doublet ascribed to $Cu_6Fe_3O_7$, viz., 1.00 mm/s is, however, higher than that for delafossite phase, viz., 0.67 mm/s. More sharper electric-field gradients due to higher density may be the cause of the higher quadrupole splitting. The fact that some Fe^{2+} species can be introduced in the fit could reinforce the attribution of this doublet to $Cu_6Fe_3O_7$. However, its large quadrupole splitting can also be due to nonstoichiometric or defected delafossite.

In a very recent paper Smith and Goodenough[21] have established a linear dependence of the isomer shift on the bond length for Fe^{3+} and Fe^{2+} in microdoped monoxides (MO's). However, an increase of covalent Fe-O σ bonding (either by bending of the 180° Fe-O-Fe bond or by introducing more electropositive counter cation M in the 180° Fe-O-M bonds) could decrease the IS. From their linear relationship and our observed IS=0.35 mm/s which is typical for Fe^{3+} in a sixfold oxygen coordination, a bond length of $\sim$1.93 Å could be deduced for the $Cu_6Fe_3O_7$ phase if inductive effects are not considered. Insofar as a fit employing the two doublets for this phase is concerned, the IS=0.67(14) mm/s should correspond to Fe^{2+} in tetrahedral oxygen coordination. However, the rather low value of this IS (with reference to the value expected from the linear relationship) implies a bending of the Fe-O-Cu bond from 180° to nearly 90°. These systematics could help evolve a clear picture about the precise atomic arrangements in the $Cu_6Fe_3O_7$ system, which is known to belong to the hexagonal family and possess an x-ray-diffraction pattern closely similar to that reported for delafossite phase. Indeed, the present study has once again brought into focus the issues of existence and stability of $Cu_2OFe_2O_3$ (delafossite) and $3Cu_2OFe_3O_4$ ($Cu_6Fe_3O_7$) phases in the Cu-Fe-O phase diagram.

It may be noted from Table I of hyperfine parameters that in the CuO sample implanted at low dose, in addition to the doublet ascribed to $Cu_6Fe_3O_7$ there is another doublet with the same isomer shift but with a much higher (1.5 mm/s) quadrupole splitting. This doublet is not observed in the sample implanted at higher dose. It seems that in the low-dose-implanted sample, the point defects are present within the $Cu_6Fe_3O_7$ configuration and these are eliminated by further implantation.

In the Cu_2O sample implanted at 2×10^{16} ions/cm^2 one has a small Fe^{2+} contribution in addition to the doublet corresponding to the $Cu_6Fe_3O_7$ phase. Gries, Sawicka, and Sawicki[7] have ascribed the occurrence of Fe^{2+} state in their internal oxidation study of Fe in Cu to quasimolecular units of the form Cu_2OFeO, wherein two Cu^+ ions are substituted by one Fe^{2+} ion. It has been argued that the smaller ionic radius of Fe can lead to significant reduction of the compressive stress and should be energetically favorable. The isomer shift in our case, viz., 1.09 mm/s is, however, much smaller than that ascribed to the quasimolecular units of Cu_2OFeO by Gries, Sawicka, and Sawicki,[7] viz., 1.66 mm/s. Such difference may be due to the fact that in the as-implanted state a good definition of the structural units may not result. It is interesting to note that the hyperfine parameters found for samples implanted at 2×10^{16} ions/cm^2 (IS=1.09 mm/s, QS=2.12 mm/s) and at 5×10^{16} ions/cm^2 (IS=1.09 mm/s, QS=1.80 mm/s) are in a very good agreement with those found by Roset and Fernandez[22] for ^{57}Co-doped Cu_2O heated at 1000 °C (IS=1.11 mm/s, QS=2.21 mm/s) and at 800 °C (IS=1.06 mm/s, QS=1.80 mm/s), respectively. Since this is only a small contribution in the spectrum (4.5%) and, since it exists only in the as-implanted state, we do not discuss it further.

Among the different cases of as-implanted states, the case of high-dose implantation in Cu_2O is perhaps the most interesting because it shows the presence of two magnetic sextet contributions in addition to the quadrupole split doublets. These sextets can be identified with the $Cu_xFe_{3-x}O_4$ ferrite phase. If one attempts to balance the chemical equation for stoichiometry with Cu_2O and Fe, on one hand, and $Cu_6Fe_3O_7$ and $Cu_xFe_{3-x}O_4$ with a small Fe^{2+} contribution, on the other, it becomes essential to assume that some free Cu should result due to the implantation. This can indeed be seen from x-ray data. It is interesting to see that a deficiency of oxygen compounded with enhancement in the concentration of Fe atoms leads to evolution of a ferromagnetic correlation in the system.

The effects of annealing of the ^{57}Fe implanted CuO sample at 400 and 500 °C can be interpreted in the following way. In the low-dose implanted case, the annealing leads to complete elimination of the doublet having a large quadrupole splitting (which was attributed to the disordered $Cu_6Fe_3O_7$ or delafossite phase), a significant reduction of the doublet assigned to the $Cu_6Fe_3O_7$ phase with a concomitant emergence of a significant contribution of the delafossite phase ($CuFeO_2$). Such a transformation can be accounted for in terms of the internal oxidation of the $Cu_6Fe_3O_7$ phase promoted by the oxygen secondaries that are generally created and are deposited during the implantation process.

Thus,

$$2Cu_6Fe_3O_7+O(\text{secondaries})\rightarrow 6CuFeO_2+3Cu_2O\ . \quad (1)$$

The cuprous oxide thus generated can only be seen in the XRD spectra, since it is not Mössbauer addressable. In the high-dose implanted CuO case, the same type of transformation is observed upon annealing at 400 °C. In fact, in this case a single phase $CuFeO_2$ material is formed.

When the implanted CuO samples are annealed at 500 °C, the delafossite phase is seen to transform partially along the following routes.

$$2CuFeO_2 \rightarrow Fe_2O_3 + Cu_2O \ , \quad (2)$$

$$3CuFeO_2 \rightarrow CuFe_2O_4 + 2CuO + Fe \ . \quad (3)$$

Thus, after annealing at 500 °C, one ends up with the following Mössbauer addressable phases: $CuFeO_2$, Fe (small clusters), α-Fe_2O_3, and $Cu_xFe_{3-x}O_4$ (ferrite). The negative isomer shift for the iron clusters indicates that probably the structure of iron is fcc. Some quantities of cupric and cuprous oxides must also be released in the process, and this is revealed by the XRD results. It may be noted that in the low-dose-implanted case, the remaining 18% contribution of the $Cu_6Fe_3O_7$ phase after annealing at 400 °C would first complete its transformation as per Eq. (1) and would then follow the routes given by Eqs. (2) and (3).

After annealing at the higher temperature, α-Fe_2O_3 disappears. As proposed by B. Lerebours *et al.*,[23] hematite can react with cuprous oxide to give a ferrite as per the equation $Cu_2O + 5Fe_2O_3 \rightarrow 4Cu_{0.5}Fe_{2.5}O_4$. The low values obtained for the hyperfine fields can be explained by the presence of monovalent copper in the tetrahedral sites of the ferrite. The presence of Cu^1 will favor the transformation $Cu^{2+} + Fe^{2+} \rightarrow Cu^{+} + Fe^{3+}$, explaining why Fe^{3+} is mainly detected in the magnetic patterns.

In the case of the ion-implanted Cu_2O system, the annealing treatment shows somewhat different trends as compared to the CuO case. The difference in the behavior should correspond to the difference in the stoichiometry. In the case of the low-dose-implanted Cu_2O samples, annealing at 400 °C transforms the $Cu_6Fe_3O_7$ and Fe_2O_3 and $Cu_xFe_{3-x}O_4$ phases. The Fe^{2+} state probably associated with a quasimolecular metastable complex is also transformed completely. The reaction routes followed in this case should be similar to the ones given by Eqs. (1), (2), and (3). However, since the small contribution of Fe reflected by Eq. (3) is not observed in the low- and the high-dose-implanted Cu_2O samples, some modification of the route suggested earlier for the formation of Fe_2O_3 and $CuFe_2O_4$ phases appears to have resulted. The possibility in this case is discussed below.

When the low- and high-dose-implanted Cu_2O samples are annealed at 500 °C, one basically observes a clear increase in the contribution of the delafossite ($CuFeO_2$) phase, which is associated with the transformations in Fe_2O_3 and $CuFe_2O_4$ along with an emergence of a small contribution of Fe clusters. The $Cu_6Fe_3O_7$ phase is seen to be eliminated completely. In the low-dose situation, Eqs. (1) and (3) are seen to be operative with a total conversion of $Cu_6Fe_3O_7$ into delafossite ($CuFeO_2$) and a partial conversion of delafossite into $CuFe_2O_4$ (which increases from 19–28 %) and Fe clusters (5%). In the high-dose-implanted Cu_2O sample, however, Fe_2O_3 and $CuFe_2O_4$ are seen to reduce substantially along with elimination of the small contribution of $Cu_6Fe_3O_7$. Concomitantly, there is a substantial increase in the contribution of $CuFeO_2$ and the appearance of a small quantity of Fe clusters.

Since the reduction in the contributions of $CuFe_2O_4$ and Fe_2O_3 is roughly in the ratio of 2:1 (see Table III), one formula unit of Fe_2O_3 is seen to be consumed for two formula units of $CuFe_2O_4$ in the presence of Cu_2O matrix available in the proximity for the reaction. Thus, the reaction of the following type can be conceived;

$$4Cu_2O + 4CuFe_2O_4 + 2Fe_2O_3 \rightarrow 12CuFeO_2 + O_2 \ . \quad (4)$$

Even though the annealing is performed in the argon atmosphere, this system configuration seems to be susceptible for some intrinsic reduction. The appearance of a small number of Fe clusters can result if the mechanism given in Eq. (3) is partially operative, presumably in the subsurface region. This mechanism is fully confirmed when the low-dose-implanted sample is annealed at 600 °C. This is not the case for the high-dose-implanted sample, for which a doublet due to Fe^{3+} in a tetrahedral or very distorted site is detected.

From the entire discussion given above it becomes clear that the Cu-Fe-O system drives itself into the delafossite ($CuFeO_2$) configuration upon thermal annealing treatment. However, as demonstrated by Dimitrov, Bojanov, and Nicolov[24] in a study of the interaction of the CuO-Fe_3O_4 and Cu_2O-Fe_3O_4 systems, the CuO dissociation is a comparatively slower process and longer heating is necessary to fully obtain $CuFeO_2$. This is confirmed by the larger numbers of magnetic phases after heating at 600 °C in CuO samples than occurred in Cu_2O.

Smith *et al.*[9] have compared the hyperfine parameters for different material systems involving Cu-O coordination, such as $BaCu_{0.0997}Fe_{0.003}O_2$, $Y_2BaCu_{0.997}Fe_{0.003}O_5$, $CaFeO_3$, CuO(^{57}Co), $La_2Cu_{0.995}Fe_{0.005}O_4$, and $YBa_2(Cu_{0.998}Fe_{0.002})_3O_7$. Among these, the parameters corresponding to the Cu(2) pyramidal site, viz., IS=0.32 mm/s and QS=0.62 mm/s, match those observed in the present study in the case of $CuFeO_2$. In a recent work of Marest and Bagglo-Saitovitch[25] a similar doublet (IS=0.25 mm/s, QS=0.65 mm/s) was found for ^{57}Fe-implanted $YBa_2Cu_3O_{7-\delta}$. It was assumed to be due to the occupation of the Cu(2) site. Another doublet (IS=0.23 mm/s, QS=1.51 mm/s) similar to the doublet D_2 present in the CuO sample implanted at 2×10^{16} ions/cm^2 was also detected. This doublet reflects a highly disordered local environment for iron. It is characteristic of reduced $YBa_2Cu_3O_{7-\delta}$ samples and would be due to the planar oxygen configuration determined for the Cu ions in the Cu(1) site in the orthorhombic phase. Analysis to identify the reason for such similarity is being performed.

CONCLUSION

A systematic study on ^{57}Fe ion implantation in cupric and cuprous oxide films has been reported. It has been found that in case of cuprous oxide samples, phases such as $CuFeO_2$, β-$CuFeO_2$ and $Cu_6Fe_3O_7$ are observed after implantation. After annealing it has been observed that contribution of $Cu_6Fe_3O_7$ phase continuously decreases at the benefit of $CuFeO_2$. In the case of Cu_2O, annealing at 400 °C is found to favor the formation of magnetic $CuFe_2O_4$. After annealings at 500 and 600 °C both samples (implanted cupric and cuprous oxide) showed formation of paramagnetic iron particles.

ACKNOWLEDGMENTS

The authors would like to thank Dr. B. Hannoyer of the University of Rouen (France) for valuable discussions and A. Plantier who performed implantations on the isotope separator of the IPN Lyon. The authors wish to gratefully acknowledge the financial support by Indo French Centre for the Promotion of Advanced Research (IFCPAR)/Centre Franco-Indien pour la Promotion de la Recherche avancee (CEFIPRA) for carrying out this work under the research Programme No. IFC/308-2.

[1]W. Ronald Cares and J. W. Hightower, J. Catal. **39**, 36 (1975).
[2]M. Bhaduri, J. Chem. Phys. **75**, 3674 (1981).
[3]J. Janicki, J. Pieterzak, A. Porebska, and J. Suwalski, Phys. Status Solidi A **72**, 95 (1982).
[4]B. Hannoyer, J. Durr, G. Calas, J. Petiau, and M. Lenglet, *Proceedings of the Second European Conference "Studies in Inorganic Chemistry"* [Solid State Chem. **3**, 551 (1983)].
[5]B. Hannoyer, M. Lenglet, R. Chopova, and J. C. Tellier, Mater. Chem. Phys. **13**, 449 (1985).
[6]M. Bhaduri, J. Chem. Phys. **77**, 1400 (1982).
[7]W. H. Gries, B. D. Sawicka, and J. A. Sawicki, Nucl. Instrum. Methods B **18**, 291 (1987).
[8]Ch. Niedermayer, A. Golnik, E. Recknagel, M. Rossmanith, A. Weidinger, L. Takacs, A. Teh, G. Zhang, and C. Hohenemser, Phys. Rev. B **38**, 2836 (1988).
[9]M. G. Smith, R. D. Taylor, M. P. Pasternak, and H. Oesterreicher, Phys. Rev. B **42**, 2188 (1990).
[10]A. Barcs, L. Bottyan, B. Molnar, D. L. Nagy, N. S. Ovanesyan, and H. Spiering, Hyperfine Interact. **55**, 1187 (1990).
[11]M. Sohma and K. Kawaguchi, Solid State Commun. **79**, 47 (1991).
[12]P. Shah and A. Gupta, Phys. Rev. B **45**, 483 (1992).
[13]S. B. Ogale, P. G. Bilurkar, N. Mate, S. M. Kanetkar, N. Parikh, and B. Patnaik, J. Appl. Phys. **72**, 3765 (1992).
[14]Ion implantations and conversion electron Mössbauer analysis were carried out at the Institute de Physique Nucleairc, Lyon, France.
[15]G. Le Caer and J. M. Dubois, J. Phys. E **12**, 1983 (1979).
[16]Glancing-angles x rays were carried out at the Department of Physics, University of Poona, India.
[17]M. Bhaduri, J. Chem. Phys. **75**, 3674 (1981).
[18]B. Hannoyer, these de Doctorat d'Etat, Universite' de Rouen, 1983.
[19]A. H. Muir and H. Wiedersich, J. Phys. Chem. Solids **28**, 6 (1967).
[20]D. S. Buist, A. M. M. Gadalla, and J. White, Mineral. Mag. **103**, 731 (1966).
[21]M. G. Smith and J. B. Goodenough, J. Solid State Chem. **103**, 25 (1993).
[22]J. Roset and A. Fernandez, Phys. Status Solidi B **34**, 297 (1986).
[23]B. Lerebours, J. Durr, A. d'lluisser, J. P. Bonnelle, and M. Lenglet, Phys. Status Solidi A **61**, 75 (1980).
[24]R. Dimitrov, B. Bojanov, and S. Nicolov, Thermochim. Acta **34**, 149 (1979).
[25]G. Marest and E. Baggio-Saitovitch, Hyperfine Interact. **66**, 401 (1991).